PROGRESS OF THE ROLLER-PRINTING METALLISATION TECHNIQUE TOWARDS AN INDUSTRIALLY COMPATIBLE ALTERNATIVE TO SCREEN PRINTING

F. Huster, M. Spiegel, P. Fath, E. Bucher
Universität Konstanz, Fachbereich Physik, Fach X916, 78457 Konstanz
Tel.: +49-7531-88-2074, Fax: +49-7531-88-3895
E-mail: frank.huster@uni-konstanz.de

T. Denner, K. Schanz
EKRA GmbH, Zeppelinstrasse 16, 74357 Bönnigheim, Germany

ABSTRACT: Roller-printing of metallisation paste to form the contact grid on mechanically textured surfaces represents a novel and promising technique with the ability to surpass conventional screen-printing in many aspects. It is well suited for the integration into industrial production lines due to the possibility to simply replace the screen-printing step by the high-throughput in-line roller-printing step. The printing areas are defined in the mechanical texturisation step simultaneously with the formation of V-grooves for reduced reflection. Roller-printed contact fingers possess a remarkable combination of low shadowing losses (optical finger width of 30 μm) with good conduction properties (finger cross-section 600 μm^2, contact width 120 μm), that lies in the range of the contact fingers of buried contact solar cells. Cell efficiencies up to η=14.6% with a series resistance of only 0.2 Ωcm^2 have been obtained on 100 cm^2 multi-crystalline material in a PECVD-SiN firing-through standard process with a 30Ω/sq emitter. Calculations predict an efficiency gain of 0.8% abs. of roller-printed cells compared to screen-printed cells on a 50 Ω/sq-emitter with an optimised finger spacing.
Keywords: Roller-printing - 1: Metallisation - 2: Multi-crystalline - 3

1. INTRODUCTION

Screen-printing of metallisation pastes for contact formation on solar cells is the predominant technology currently used in industrial production lines. As this technology will meet its limits in future industrial developments (e.g. very high throughput) and economic needs (cost reduction), it is time for a novel metallisation technique like roller-printing to enter the scene.

The concept of roller-printing has been presented the first time by our group in 1994 [1], and results of hand-roller printed cells followed in 1995 [2]. After some years without strong efforts on improving roller-printing we began in 1998 to develop both a roller-printing apparatus and an adapted process to implement this technique into industrial production lines. Now we are able to present the first promising results obtained with this new apparatus.

2. THE ROLLER-PRINTING TECHNIQUE

2.1 Concept

There are various possibilities for the application of a rotational printing technique within a solar cell process: front side metallisation (contact grid), back side metallisation (full area or pattern), deposition of dopant pastes or masking resists etc. At the University of Konstanz we currently focus on the finger printing on mechanically textured cells. The underlying idea is to define the printing areas (i.e. the contact fingers) of the front grid solely by appropriately grinding the wafer surface, using mechanical texturisation with rotating abrasive wheels. In the printing step the protruding regions are covered with metallisation paste by an even wheel, as shown in Figure 1. The busbars are formed by dispensing paste stripes perpendicular to the fingers.
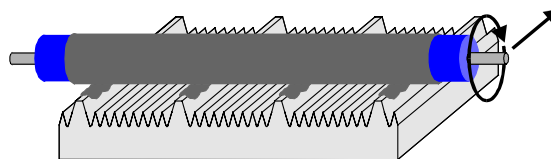

Figure 1: *Roller-printing technique on mechanically textured surfaces*

2.2 Features

In many aspects roller-printing has the potential to outperform conventional screen-printing due to the following features:

- High throughput exceeding 1200 wafers/hour
- Mask-free in-line technique, therefore well suited for the implementation into production lines. Continuous printing with high uptimes is expected.
- Self-alignment property: Because the fingers are defined by the surface texturing no delicate alignment step is needed as it is in the case of screen-printing on mechanically textured wafers. This property also enables an easy application of a selective emitter by roller-printing of a diffusion source on the contact areas (fingers) for the heavy diffusion. The shallow diffusion for the light-active regions between the fingers can be realised by POCl$_3$-diffusion, by second roller-printing of a diffusion source or simply by outdiffusion from the diffusion source on the fingers [3].
- Superior geometrical finger characteristics: small optical finger widths down to 30 μm, large cross-sections comparable to screen-printed fingers and even enhanced contact widths. These geometrical characteristics are especially important for contacting shallow, lowly doped emitters.

2.3 Process

Roller-printing can easily be integrated into an industrially compatible process as a substitution for screen-printing, like it is done in our case and displayed in Figure 2.
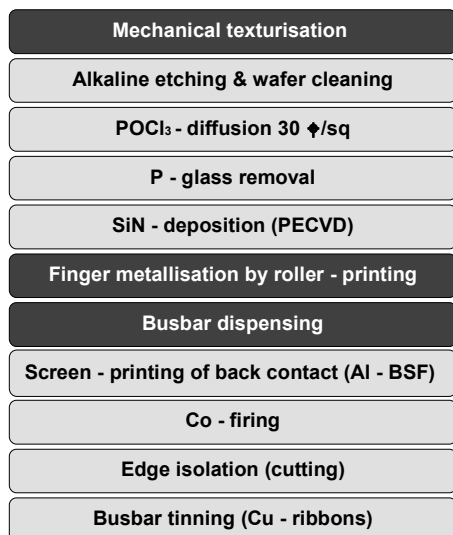
Figure 2: Process sequence
- Mechanical texturisation
- Alkaline etching & wafer cleaning
- POCl$_3$ - diffusion 30 ♦/sq
- P - glass removal
- SiN - deposition (PECVD)
- Finger metallisation by roller - printing
- Busbar dispensing
- Screen - printing of back contact (Al - BSF)
- Co - firing
- Edge isolation (cutting)
- Busbar tinning (Cu - ribbons)

Figure 2: *Process sequence including roller-printing. Dark highlighted steps are specific for or adapted to roller-printing.*

In the following subsections the process steps that are important for roller-printing are described in detail:

2.3.1 Mechanical texturisation

The forming of protruding regions needed for roller-printing is performed simultaneously with the mechanical texturisation for reduced reflectance, light trapping and enhanced charge carrier collection probability. To investigate a broad variety of surface profiles, which are crucial for the properties of the metallized fingers, most of the mechanical texturisation was carried out by using a single blade. When the best profile is evaluated a texturing wheel for roller-printed cells will be manufactured. A typical roller-printing profile is shown in Fig. 3; to avoid metallisation of the light-active areas between the fingers an elevation of 50 µm of the finger tips above the remaining areas is needed.
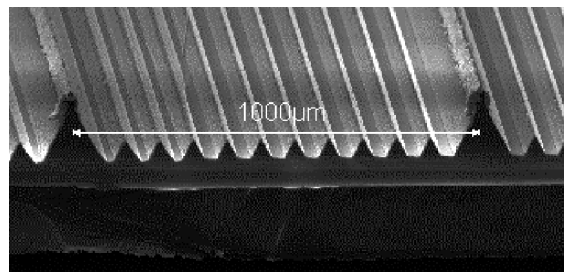
Figure 3: *SEM picture of a profile suitable for roller-printing; fingers are already metallized.*

2.3.2 Roller-printing and drying

The paste film on the printing wheel of the roller-printing apparatus is adjusted to a thickness between 20 µm and 30 µm. A commercially available silver paste is used without viscosity modifications. Thanks to its self-alignment property it is possible to apply several printing steps, whereby uniform and low resistive fingers are obtained. The number of printing steps has been reduced from 6 at the beginning down to 2 by a suitable choice of rubber hardness and a fine tuning of the contact pressure and the film thickness. A drying time of 10 seconds between these 2 printing steps, corresponding to furnace length about 1 m, emerged to be sufficient.

2.3.3 Busbar dispensing

The busbars are dispensed and subsequently reduced in height by another passage through the roller-printing apparatus. This helps to avoid a too strong shrinking of the busbars which would lead to their separation from the fingers in the firing step.

2.3.4 Back side

The back side metallisation is done by screen-printing for simplicity, but will be replaced by a roller-printing metallisation later.

2.3.5 Anneal

Due to the small quantities of roller-printed solar cells processed so far no thorough firing optimisation has been performed to take into account the reduced surface reflection and also the smaller wafer thickness. Therefore most of the cells were treated in an annealing step in forming gas (Ar/H$_2$) to reduce contact resistance.

2.3.6 Tabbing

The currently not satisfying performance of the busbar dispensing (interruptions at the finger tips) necessitates a busbar tabbing with copper ribbons, as seen in Figure 4.
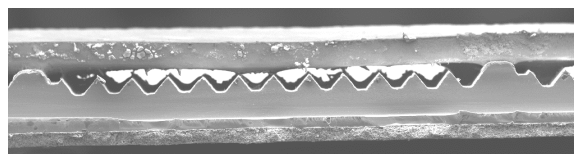
Figure 4: *Copper ribbon for enforcement of the busbar*

3. CELL RESULTS

On 10x10 cm^2 multi-crystalline material (Baysix) the results displayed in Table I have been obtained by applying the standard process described in section 2.3. For the roller-printed cells finger profile V (finger spacing 1 mm) was formed using single blade texturisation (see also section 4). Comparing the average results of 3 roller-printed cells with the results of the reference cells one observes an increase of J$_{sc}$ (+1.2 mA/cm^2/ 4%), which can be attributed to the surface texturing as well as a decrease in V$_{oc}$ (-11 mV). The normally observed fill factor loss due to the surface enlargement (around 1.5% absolute in this case of 1.8 as enlargement factor) is overcompensated by the reduced series resistance of the roller printed cells. The shadowing losses are the same for both groups:
- Roller-printed cells: 40 µm optical finger width and 1 mm finger spacing corresponds to 4% finger shadowing losses.
- Screen-printed cells: 120 µm finger width and 3 mm spacing also adds up to 4% shadowing losses.

Type / quantity	Anneal Ar/H$_2$	FF %	J$_{SC}$ mA/cm^2	V$_{OC}$ mV	η %
Roller-printed Best cell	yes	77.7	31.4	599	**14.6**
Roller-printed Average 3 cells	yes	77.3	31.3	599	**14.5**
Roller-printed Average 3 cells	no	74.4	31.9	599	**14.2**
Reference: Untextured and screen-printed Average 2 cells	yes	77.1	30.1	610	**14.1**

Table I: *Cell results*

4. FINGER PROFILE AND PRINTING OPTIMISATION

The performance of roller-printing as a printing technique is mainly quantified by the properties of the printed fingers, i.e. shadowing losses and series resistance contributions. The geometrical finger parameters determining these properties are the following:

- optical width
- cross-section
- contact width

Standard screen-printed fingers have a finger width and therefore also a contact width of about 120 µm and a cross-section of roughly 1000 µm^2. By profiling the areas carrying the metallisation as it is done in the texturisation step of the roller-printing process the proportion of the optical finger width to the contact width and also to the cross-section can be improved. This improvement leads to reduced shadowing losses and at the same time lower series resistances.

In Table II five investigated finger profiles are listed as scanning electron microscope (SEM) pictures together with their finger characteristics. The wheel-textured profile I was used in the first generation of roller-printed cells. Profiles II and III show contact widths and cross-sections

in the range of screen-printed standards and at the same time noticeably lower optical widths. Types IV and V as high-performance profiles indicate the high potential of roller-printed contacts. Especially profile V leads to excellent finger characteristics comparable to those of buried contact cells. On laboratory scale shunting of cells with this profile has not been a problem yet, but for industrial production profile II might be the best compromise to form small fingers in a reliable manner.

The profiles II - V displayed in table II are obtained by using a 60°-dicing blade and an etching time between 2 and 5 minutes in 80°C NaOH-solution.

The number of printing steps has been reduced from 6 down to 2 by an optimisation of the printing parameters. This appears to be the optimal number because on one side the roller-printing and drying can be done in an apparatus of about 3 m in length (2 printing and 2 drying units, for a throughput above 1200 wafers/hour) and on the other side this ensures a homogenous paste deposition without finger interruptions.

5. SERIES RESISTANCE INVESTIGATIONS

5.1 IV-Characterisation and series resistance analysis

To verify the good conducting properties of the roller-printed fingers of profile V a series resistance analysis on three exemplary cells, from each group of Table I, is carried out: RP_{an} (roller-printed, annealed), RP (without anneal), and SP_{an} (screen-printed reference, annealed).

First the main series resistance contributions are measured separately (Table III; note the similarity of $R_{contact}$ of RP_{an} and SP_{an}, indicating that the contact width of the roller-printed cell is indeed about 120 µm).

Second they are summed up to a lumped series resistance, considering the grid geometry (1 mm finger spacing for the RP-cells, 3 mm for the SP-cell, 2 busbars). These calculated contributions are listed in Table IV, showing the summarised series resistance of the RP_{an}-cell to be only 1/3 of the resistance of the SP_{an}-cell (column 3).

Profile	I	II	III	IV	V
Texturing tool	Wheel	Single blade	Single blade	Single blade	**Single blade**
Finger:					
Optical width [µm]	140	85	70	30	**30**
Contact width [µm]	200	200	130	90	**120**
Cross-section [µm^2]	1600	1000	650	350	**600**
Line resistance [mΩ/cm]	550	350	550	1000	**600**

Table II: *Investigated roller-printed finger profiles. Type I through IV are 6 times printed, which has been reduced for type V to 2 times. The optical width and contact width are estimated from the SEM pictures (optical width confirmed by analysis of light microscope pictures), whereas the cross-section is calculated from finger line resistance measurements supposing a resistivity of 3.5 µΩ cm of the silver paste.*

Cell	$R_{emitter}$ (sheet resistance)	$R_{contact}$	R_{line} (finger resistance)
	Ω/sq	mΩ cm^2	mΩ/cm
RP$_{an}$	24*	2.8	730
RP	27*	16.6	720
SP$_{an}$	28	2.6	730

Table III: *Resistances measured by the transfer length method [4] ($R_{emitter}$ and $R_{contact}$) and by four-point-probing (R_{line}). The sheet resistances marked with (*) are calculated from the measurement by dividing by 1.8 (surface enlargement factor). For $R_{contact}$ a contact width of 120 μm was assumed for all cells.*

Cell	$R_{emitter}$	$R_{contact}$	R_{line}	Busbar +basis	Sum R_{series}
	Ω cm^2	Ω cm^2	Ω cm^2	Ω cm^2	Ω cm^2
RP$_{an}$	0.037	0.024	0.146	0.04	0.25
RP	0.041	0.142	0,144	0.04	0.37
SP$_{an}$	0.212	0.066	0.425	0.05	0.75

Table IV: *Calculated series resistance contributions based on the measurements displayed in Table III.*

Finally these calculated series resistances are compared to those extracted from IV-measurements as seen in Table V.

Cell	FF	J_{01}	J_{02}	R_{shunt}	R_{series}
	%	10^{-12} A/cm^2	10^{-8} A/cm^2	Ωcm^2	Ωcm^2
RP$_{an}$	77.2	1.49	(9)[1]	5000	0.18
RP	75.0	1.60	(9)[1]	3500	0.44
SP$_{an}$	76.9	1.18	(5)[1]	4000	0.63[2]

Table V: *Cell parameters extracted from dark and illuminated IV measurements using a 2-diode-model fit with $n_1=1$ and $n_2=2$.*

There is a good conformity of the values of R_{series} obtained from the calculation on one side and from the fitting of the IV-measurements on the other. The difference of approx. 0.5 Ωcm^2 between R_{series} of *RP$_{an}$* and *SP$_{an}$* corresponds to a fill factor increase of 2% abs., therefore overcompensating the fill factor loss of 1.5% abs. by the enlargement of the space charge region due to the surface texturing. The very low values of $R_{emitter}$ and $R_{contact}$ of *RP$_{an}$* emphasize its suitability for contacting lowly doped emitters.

5.1 Calculation of possible efficiency gains

To show the full potential of roller-printing a calculation of the efficiency gain when applying it on a higher-ohmic emitter is useful.

---

[1] J_{02} was held fixed at reasonable values (taking into account the enlargement factor of 1.8 for the textured cells), because the IV-measurements showed some deviations from ideal 2-diode behaviour between 0 V and 0.5 V.

[2] This series resistance exhibits a high ratio of a distributed behaviour (~90%) in accordance with the proportions of the resistances in Table V. For further details on the evaluation of IV-characteristics see [5].

The calculations are based on the following assumptions:

- $R_{emitter}$ = 50 Ω/sq, $R_{contact}$ = 10 mΩcm^2
- Two busbars; finger geometry according to Table II
- Surface enlargement factor of 1.8 for all cells
- 2-diode-model for evaluating J_{sc}, FF and η, using $J_{01} = 1.5 \cdot 10^{-12}$ A/cm^2, $J_{02} = 9 \cdot 10^{-8}$ A/cm^2, $n_1=1$, $n_2=2$, R_{shunt} = 10000 Ωcm^2

Cell/ Profile	d_{opt}	R_{series}	Sh-loss (finger)	FF	J_{sc}	η
	mm	Ωcm^2	%	%	mA/cm^2	%
SP	2	0.64	5.8	75.4	31.9	14.5
RP/II	1.9	0.54	4.2	75.8	32.5	14.8
RP/V	1.2	0.39	2.4	76.5	33.1	15.3

Table VI: *Calculated efficiency gain with optimised finger distance d_{opt} on a 50 Ω/sq-emitter. J_{sc}-differences are calculated from the shadowing losses (Sh-loss).*

6. CONCLUSIONS AND OUTLOOK

Roller-printing as a novel technique for printing contact grids on solar cells has been shown to be superior to screen-printing. Finger widths down to 30 μm were obtained with low line resistances and large contact areas. Cell efficiencies up to 14.6% has been obtained that are at least comparable to screen-printed references.

As it is indicated by the calculations the roller-printing technique will show its full potential when applying it on lowly doped emitters, where efficiency gains of 0.8% abs. compared to screen-printed references can be expected. The next innovation step will be the integration of a selective emitter also formed by roller-printing to establish an industrially compatible highly efficient process.

7. ACKNOWLEDGEMENTS

8. REFERENCES

[1] G. Willeke and P. Fath, Proc. 12th EC PVSEC, Amsterdam 1994, 766

[2] P. Fath, C. Marckmann, E. Bucher, G. Willeke; J. Szlufcik, K. de Clerq, F. Duerinckx, L. Frisson, J. Nijs, and R. Mertens, Proc. 13th EC PVSEC, Nice 1995, 29

[3] J. Horzel, J. Szlufcik, M. Honore, J. Nijs, and R. Mertens, Proc. 14th EC PVSEC, Barcelona 1997, 61

[4] D. Meier and D. Schroder, IEEE Transactions on Electron Devices ED-31, 1984, no.5, 647

[5] B. Fischer, P. Fath, and E. Bucher, this conference